Development of a Separable 3D Cell Co-Culture System for the Study of Stem Cell Microenvironments

A Thesis

Presented to

The Academic Faculty

By

Nathaniel Bloodworth

Georgia Institute of Technology

School of Biomedical Engineering

December 2010

ACKNOWLEDGEMENTS

This work is dedicated to my research mentor, Dr. Johnna Temenoff, as well as my graduate student mentor, Taymour Hammoudi, for their invaluable assistance, direction, and most of all patience in my continuous struggle to learn how to be a scientist. Additionally, I would like to thank all the members of the Temenoff laboratory, Derek Doroski, Peter Yang, Jeremy Lim, Sharon Hamilton, Song Seto, Yongzhi Qiu, and Taymour Hammoudi, as well as Dr. Hang Lu, for your guidance, mentorship, and friendship. I have learned something from each of you, and I will dearly miss all of you.

The author would also like to acknowledge the funding provided by the Petit Undergraduate Research Scholars award.

Some of the materials employed in this work were provided by the Texas A&M Health Science Center College of Medicine Institute for Regenerative Medicine at Scott & White through a grant from NCRR (NIH P40RR017447).

TABLE OF CONTENTS

	Page
List of Figures	4
List of Abbreviations	5
Summary	6
Introduction	7
Necessity of an in vitro tissue model and important factors in its design	8
Hydrogels are an ideal candidate for an artificial extracellular matrix in 3D cell culture	8
Photolithographic methods allow for the controlled patterning of spatially defined hydrogel constructs	9
Summary of the development and optimization of the 3D co-culture system	11
Materials and Methods	13
Synthesis, purification, and characterization of the oligo(poly(ethylene glycol) fumarate) and poly(ethylene glycol) diacrylate polymers	13
Synthesis, purification, and characterization of the chondroitin sulfate methacrylate polymer	14
CSMA hydrogel characterization: fold swelling ratio and degradation time	14
Fabrication of microfluidic devices and photolithography masks	15
Hydrogel photopatterning optimization: OPF/PEG-DA and CSMA	16
System optimization: flow cell washing	18
System optimization: hydrogel lamination and demonstration interface stability and separability through the incorporation of a degradable CSMA adhesive	19

Creation and degradation of a hydrogel tri-laminate with a degradable CSMA interface, and assessment of cell population segregation and viability before and after degradation 20

Results 21

CSMA hydrogel characterization: fold swelling ratio and degradation time 21

Hydrogel photopatterning optimization: OPF/PEG-DA and CSMA 22

System optimization: flow cell washing 24

System optimization: hydrogel lamination and demonstration interface stability and separability through the incorporation of a degradable CSMA adhesive 25

Creation and degradation of a hydrogel tri-laminate with a degradable CSMA interface, and assessment of cell population segregation and viability before and after degradation 26

Discussion 27

Conclusion 31

References 32

LIST OF FIGURES

		Page
Figure 1:	A hydrogel structure created through the sequential photopatterning of individual components	10
Figure 2:	Visual representation of the final implementation of the system in creating a separable 3D co-culture structure	11
Figure 3:	Summary of the experimental procedure to optimize the photopatterning of OPF/PEG-DA and CSMA hydrogels	16
Figure 4:	Summary of the crosslinking chemistries for both OPF/PEG-DA hydrogels and CSMA hydrogels	16
Figure 5:	Simulated washing of cells from a microfluidic flow cell after crosslinking one set of OPF/PEG-DA hydrogels	17
Figure 6:	Creation of hydrogel tri-laminate with a degradable CSMA interface	19
Figure 7:	Plot of CSMA hydrogel degradation time as a function of fold swelling ratio	21
Figure 8:	The effects of photopatterning under nitrogen on OPF/PEG-DA hydrogel thickness, patterning fidelity, and percent increase in size after swelling	22
Figure 9:	Photopatterning of CSMA hydrogels under nitrogen	23
Figure 10:	Simulated washing of cells from a microfluidic flow cell after crosslinking one set of OPF/PEG-DA hydrogels	24
Figure 11:	Differentially swollen hydrogel laminates, and degradation of a CSMA Interface	24
Figure 12:	Creation of hydrogel tri-laminate with two segregated labeled cell populations separated with a degradable CSMA interface	25
Figure 13:	LIVE/DEAD confocal microscopy images of cells	25

LIST OF ABBREVIATIONS

ECM	Extracellular Matrix
2D	Two Dimensional
3D	Three Dimensional
PEG	Poly(ethylene glycol)
PEG-DA	Poly(ethylene glycol) diacrylate
OPF	Oligo(poly(ethylene glycol) fumarate)
CSMA	Chondroitin sulfate methacrylate
UV	Ultraviolet
TEA	Triethyl amine
DCM	Dichloromethane
FuCl	Fumaryl chloride
ANOVA	Analysis of variance
PBS	Phosphate buffered saline
PDMS	Polydimethylsiloxane
DMMB	Dimethylmethylene blue
hMSC	Human mesenchymal stem cell

SUMMARY

Stem cells represent an attractive cell choice for regenerative medicine applications due to their inherent ability to differentiate down multiple cell lineages given the correct cues. However, little is known concerning how the interactions, specifically the paracrine signaling effects, of native cells will influence the growth, proliferation, and differentiation of stem cells after implantation *in vivo*. This lack of fundamental knowledge necessitates the development of an *in vitro* model. Hydrogels are a biomaterial uniquely suited to the task of providing a tunable, cytocompatible environment in which to study these interactions between cell populations. By utilizing the technique of photolithography in conjunction with microfluidics, we developed and optimized a system to sequentially construct spatially segregated 3D co-culture constructs that will provide a basis for better understanding paracrine signaling between stem cells and other cell types native to orthopedic tissues. Additionally, by incorporating a degradable hydrogel interface between components, we demonstrated the separability of this system and the potential to isolate and recover individual populations after culture.

INTRODUCTION

Necessity of an in vitro *tissue model and important factors in its design*

The primary goal of tissue engineering is to restore and maintain tissues and organs by applying external mechanisms to encourage or augment the body's natural recuperative processes. Stem cells in particular represent an attractive cell type for these regenerative medicine applications because they are able to differentiate across a wide variety of cell lineages. However,little is known concerning the interactions between stem cells and native tissues *in vivo*. As a result, models that mimic tissues *ex vivo* have become increasingly important in the understanding of healthy tissue growth and function[1-2]. The design of these tissue models begins *in vitro* due to the high degree of control an *in vitro* experimental setting provides. In these models, environmental factors are manipulated through a variety of means to coax the cells to differentiate and replicate, taking on the form and function of the desired tissue[3].

Prominent among the numerous environmental influences affecting cell growth and function (both *in vitro* and *in vivo*) is the surrounding extra-cellular matrix (ECM), including its mechanical properties and incorporated biofactors, and soluble signaling factors from neighboring cells. Additionally, a three-dimensional (3D) environment for cell growth has proven to be critical for a proper understanding of cell function and for modeling the complexities inherent in tissue physiology[1]. The 3D culture system mimics the natural tissue environment of the cell far more effectively than the traditional 2D culture system; as a consequence the cells behave more like their *in vivo* counterparts in attributes such as migration, proliferation and apoptosis, and differentiation[4-6]. The development of a workable and accurate

tissue model will involve the implementation of several technologies in tandem to optimize these environmental factors.

In this work, a system was developed and optimized to co-culture segregated cell types in an environment that closely represents *in vivo* 3D physiology, and to allow the separation and recovery of viable cells after co-culture. To accomplish this, we first developed and optimized a set of parameters that allow for the sequential fabrication of a cell-laden construct with an adequate thickness to simulate a native tissue environment. Next, we synthesized and characterized a polymer to be incorporated as a degradable adhesive, holding multiple cell-laden constructs in close proximity and allowing for their eventual separation. Finally, we integrated each of the system components and provide proof-of-concept in our ability to create a construct with two segregated cells populations with a degradable adhesive between them allowing for their separation and recovery. The successful implementation of this system will allow future studies to discern the long-term effects on stem cell fate decisions in response to co-culture with native cell types.

Hydrogels are an ideal candidate for an artificial extracellular matrix in 3D cell culture

Culturing cells in a 3D environment normally involves seeding or encapsulating cells on or in artificial ECM scaffolding. For the artificial ECM scaffold, crosslinked networks of synthetic or biological polymers, or hydrogels, are often used. A hydrogel's capacity to retain large volumes of aqueous solution makes it an attractive candidate for an ECM, as this attribute better facilitates the exchange of soluble factors between cells in culture. Additionally, the polymers comprising the hydrogel can be chemically modified before, during, or after the

gelation process to include numerous biofactors that will further influence cell growth, migration, adhesion, and proliferation within the ECM[7-9]. The crosslinked polymers that comprise a hydrogel can be either synthetic or biological in nature; however, in order to be compatible with living systems they cannot induce cytotoxic effects on cells encapsulated within their network. Due to its non-cytotoxic and biocompatible nature, synthetic poly(ethylene)glycol (PEG) based hydrogels (such as poly(ethylene glycol)-diacrylate (PEG-DA) and oligo(poly ethylene glycol) fumarate (OPF)) have become popular choices for synthetic hydrogels in biological applications[10-13]. Additionally, PEG-based hydrogels have been shown to be conducive to the integration of various biofactors in the hydrogel network[14-15] allowing for the adjustment and fine-tuning of the ECM properties, an invaluable property when designing an *in vitro* model that would closely approximate living tissues.

In addition to the synthetic PEG-based hydrogels, hydrogels have been successfully created from derivatives of biological polymers such as hyaluronic acid[16], heparin[17], and chondroitin sulfate[18-21]. Chondroitin sulfate methacrylate (CSMA) hydrogels are of particular interest in the implementation of this co-culture system because they are readily degraded by the enzyme chondroitinase ABC lyase[22], making them an ideal candidate for a degradable adhesive to temporarily hold two or more cell populations in a close proximity.

Photolithographic methods allow for the controlled patterning of spatially defined hydrogel constructs

In the creation of an ideal tissue model, the size and shape of the construct is very important, as the exchange of soluble factors and nutrients between cells is diffusion limited due

to the lack of a vasculature. Additionally, proper spatial relationships between cells are necessary to mimic in vivo conditions[23-25], making constructs on the milimeter to microscale ideal[26]. Because milli- to micro-scale constructs are needed, a crosslinking method that would allow for microscale spatial control would be the most suitable for application in the 3D co-culture system. Numerous methods of crosslinking a synthetic or biological polymer into a hydrogel network exist, including heat molding (or thermal crosslinking), which uses heat to drive the crosslinking process; stereolithography or additive photopatterning, which uses a laser to crosslink the gel one layer at a time; and photolithography, which exposes the gel to ultra violet (UV) light to initiate polymerization[27]. Of the crosslinking techniques available for use, photolithography possesses the necessary advantage because it allows hydrogels to be photopatterned on the microscale with relatively high throughput and spatial control. In photolithography, a photomask defines the pattern to be transferred to the photosensitive polymer[28]. Transparent areas on the mask allow photons through to the polymer solution where they initiate the polymerization process, and the hydrogel forms beneath[29]. Variations on this technique have been used in the past to pattern hydrogel scaffolds in which cells are encapsulated or seeded on the surface[12, 30-32].

Whereas photolithography allows for fairly precise control of hydrogel shape, the technology of microfluidics involves the use of flow cells to study the dynamics of fluids on the micro scale. When these technologies are used in conjunction with one another, the location *and* timing of the photopolymerizable process can be controlled, allowing for the fabrication of complex 3D hydrogel constructs[33]. The temporal control imparted by the use of microfluidic flow cells also allows for the application of discrete photolithographic steps to produce multiple hydrogel components as part of a single laminated structure, as demonstrated previously by Cheung et al.[34] and shown in Figure 1. This approach to hydrogel patterning can be extended to

the patterning of cells, where different cell types are patterned in series and laminated together to form a single construct, provided the inspiration for the project.

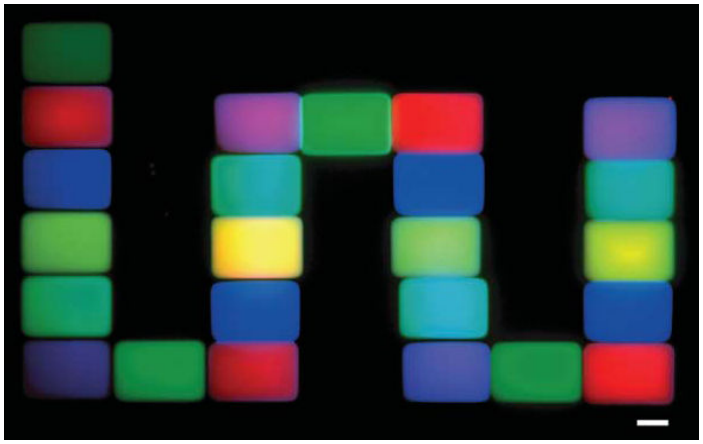

Figure 3: A hydrogel structure created through the sequential photopatterning of individual components (each shown as a different colored gel). Each gel color can be thought of as containing a different cell type, demonstrating the utility of this system in the creation of a 3D co-culture construct. Scale bar = 200 μm. Cheung et al. *Lab on a Chip* 2007.

Summary of the development and optimization of the 3D co-culture system

While the photopatterning of microscale hydrogel constructs for 3D cell culture has been achieved[35-37], current techniques are limited in their ability to produce hydrogels with thicknesses greater than 500 μm and thus do not fully recreate the thicknesses inherent in many tissues. Oxygen has been implicated previously as a potential culprit in the premature termination of the photo-polymerization process and may limit the thickness of the photopatterned hydrogels[33, 38]. The oxygen molecule's propensity to react with the free radicals that form during the polymerization reaction may cause the reaction itself to be quenched, resulting in the formation of a hydrogel with lower crosslinking density, lower patterning fidelity, and lower thickness. The first aspect of the 3D cell culture system optimized here is the photopatterning of both OPF/PEG-DA and CSMA hydrogels of sufficient thickness to model tissues by performing the crosslinking in a controlled, low oxygen environment. Additional aspects of system

development developed in this thesis are: (i) synthesizing and characterizing bulk-crosslinked CSMA hydrogel swelling and degradation properties; (ii) optimizing the sequential photopatterning process to ensure no cell types mix between crosslinking steps; (iii) combining the technologies and techniques developed in parts (i) and (ii) to create a sequentially photopatterned hydrogel structure that remains intact after swelling and that can be separated through the incorporation of a degradable CSMA interface; (iv) using techniques employed in part (iii) to create a cell-laden construct with two segregated cell populations, and separating these populations be degrading the CSMA interface between them. The final system as it would be implemented in the co-culture of multiple cell types is diagrammed in Figure 2.

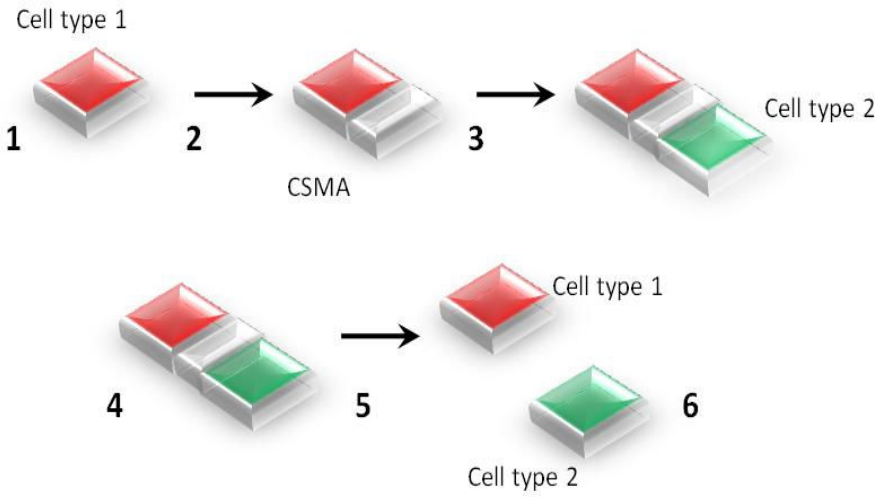

Figure 4: Visual representation of the final implementation of the system in creating a separable 3D co-culture structure. The steps are as follows: (1) A hydrogel containing cell type 1 is photopatterned (though any shape is theoretically possible, a square is shown here for illustrative purposes); (2) Residual polymer solution containing cell type 1 is removed and the degradable CSMA hydrogel adhesive is photopatterned in contact with the first hydrogel; (3) Residual CSMA polymer solution is removed and a hydrogel containing cell type 2 is photopatterned in contact with the CSMA glue; (4) The construct is placed in an environment suitable for cell growth, and the cell populations exchange soluble signaling factors with one another, influencing the behaviors of their respective counterparts; (5) The CSMA hydrogel adhesive is enzymatically degraded, separating the hydrogels containing each cell type; (6) The cell populations, now isolated, are ready to be analyzed.

MATERIALS AND METHODS

Synthesis, purification, and characterization of the oligo(poly(ethylene glycol) fumarate) and poly(ethylene glycol) diacrylate polymers

The polymer OPF was synthesized according to methods described previously[39]. A solution of Triethylamine (TEA) and fumaryl chloride (FuCl) was added dropwise to a solution of PEG dissolved in methylene chloride (MeCl; Thermo Fisher Scientific) (0.9:1 and 2:1 molar ratios of FuCl to PEG and TEA to FuCl, respectively) under Nitrogen. The addition was performed over the course of 5 hours at 4^{o}C and 2 days further at room temperature. MeCl was then removed through rotovaporation (Buchi) and TEA hydrochloride through filtration, and the OPF recrystallized in ethyl acetate, washed in ethyl ether, and vacuum dried at 25^{o}C. The final product was stored at -20^{o}C.

The PEG-DA was also prepared as previously described[40]. 0.1 mmol/mL dry PEG, 0.4 mmol/mL acryloyl chloride, and 0.2 mmol/mL TEA were combined in anhydrous dichloromethane (DCM) under nitrogen and continuous stirring and were left to react overnight. The resulting solution was washed with 2 M K_2CO_3 and separated into aqueous and DCM phases to remove any residual hydrochloric acid. The DCM phase was subsequently dried with anhydrous $MgSO_4$, and PEG-DA was precipitated in diethyl ether, filtered, and vacuum dried. The PEG-DA was stored in a sealed container at -20^{o}C and protected from light. The molecular weight distribution of both the OPF and PEG-DA was determined with gel permeation chromatography (Shimadzu).

Synthesis, purification, and characterization of the chondroitin sulfate methacrylate polymer

Chondroitin sulfate (15 g) (Sigma Aldrich) was dissolved in 60 mL of distilled/deionized H_2O (25% w/v) and heated to 60^oC with continuous stirring. Once the temperature of the reaction vessel stabilized, 60 mL of methacrylic anhydride was added dropwise at an approximate rate of ~1 mL/min. After the addition of the acrylate, 135 mL of 5 N NaOH was added dropwise at an approximate rate of ~1 mL/min. The pH of the reaction was then recorded, and the reaction was allowed to proceed for 24 h. After the completion of the reaction the pH of the solution was again recorded. The product was then precipitated in a mixture of cold methanol and isopropanol, filtered, and vacuum dried. Samples for experiments were dialyzed for three days, after which the purified solution was subsequently frozen in liquid nitrogen and dried in a lyophilizer (Labconco) for an additional four days. The product was dissolved in D_2O and characterized with H^1NMR. The synthesis was repeated and the amount of NaOH added during each repetition was varied, resulting in CSMA hydrogels with differing physical properties (see below).

CSMA hydrogel characterization: fold swelling ratio and degradation time

CSMA gel solutions for photo-crosslinking were produced through the addition of a volume of phosphate buffered saline (PBS) and 0.05% w/v D2959 photoinitiator (Ciba) to an appropriate mass of purified CSMA in order to obtain gels with compositions of 90% w/w H_2O. The gel solution was then dispersed between two glass slides (Fisher) with a 1mm separation and

exposed to UV light for 10 minutes. Individual gels of uniform size were excised and placed into PBS where they were allowed to reach their equilibrium swelling mass overnight. For the swelling studies, CSMA hydrogels were crosslinked and their equilibrium swelling masses recorded. The hydrogels were subsequently lyophilized and their dry mass measured and recorded. The fold swelling ratio was calculated by dividing the equilibrium swelling mass by the dry mass (W_s/W_d). For the degradation studies, CSMA hydrogels (90% w/w H_2O) were crosslinked in the same fashion and swollen overnight in PBS. After swelling, PBS was removed and replaced with 1.75 mL of a chondroitinase buffer solution containing Tris (50mM), sodium acetate (60 mM), and Bovine Serum Albumin (BSA, 0.02% w/v) (Sigma) at a pH of 8.0, to which 0.25 mL of the enzyme chondroitinase ABC (1 U/mL, 0.01% w/v BSA; Sigma) was added. The gels were then incubated with the enzyme at 37^{o}C and checked every 30 minutes for complete degradation. Control gels were created as well, to which 2 mL of chondroitinase buffer solution was added. The data was analyzed using one-way ANOVA followed by a Tukey-Kramer multicomparison test ($n = 5$ for the swelling studies and $n = 3$ for the degradation studies, with $\alpha = 0.01$ for both post-hoc tests).

Fabrication of microfluidic devices and photolithography masks

Photopatterning experiments were performed in a microfluidic device fabricated from polydimethylsiloxane (PDMS)[41] (Sylgard 184, Corning). Each microfluidic device was comprised of a 2 mm thick rectangular chamber in the center with three inlet and three outlet channels positioned symmetrically on either side. Prior to molding, a poly(urethane) master mold was fabricated through techniques described previously.[42] PDMS (10:1 base:curing agent ratio)

was poured over the master and allowed to cure at 70 °C for 2 h. Afterwards, the PDMS was removed from the mold, and individual devices were excised and subsequently bonded to cover glass using oxygen plasma treatment[43]. Medical grade platinum-cured silicone micro tubing was used for fluidic connections. In the inlet and outlet channels, holes for fluidic connections were punched to a size determined by the outer diameter of the tubing. The tubing was connected to the device via type 304 90°-angled stainless steel 21 gauge tubes. 21 gauge Luer lock dispensing needles were attached to the opposite ends of the tubing to allow for connection to syringes containing polymer solution. A contact-bonded, overlying PDMS enclosure was fabricated using a different poly(urethane) mold to isolate the device in a nitrogen atmosphere. Masks used in the photolithographic patterning were designed in AutoCad and printed at 10,000 dpi (CAD Art Services).

Hydrogel photopatterning optimization: OPF/PEG-DA and CSMA

Photopatterning experiments were performed in a microfluidic device fabricated from PDMS, detailed previously. The photomasks used consisted of a series of 800 μm to 3000 μm squares. Devices were equilibrated with N_2 or room air prior to loading the polymer. The photomask was aligned and the polymer solution injected and allowed to crosslink under 365 nm light for 12 min (see Figure 3). Using a dissecting microscope and ImageJ software (NIH), the dimensions of the hydrogels were measured immediately after crosslinking and after reaching equilibrium swelling. Measurements were compared using ANOVA and Tukey's post-hoc test ($n = 3$, $p \leq 0.05$). Linear regression was performed to determine the correlation between mask size and the size of the resulting hydrogel.

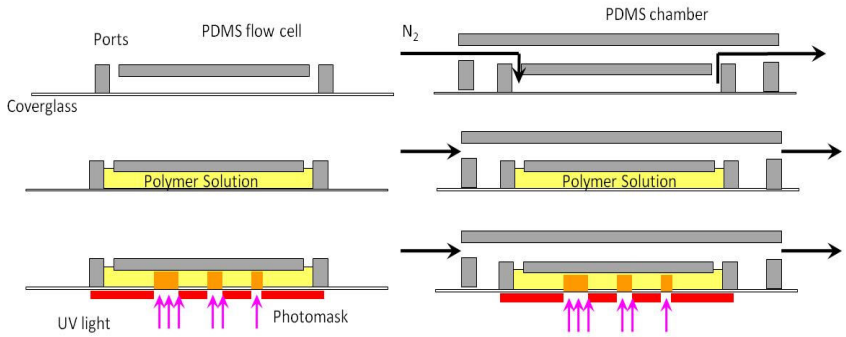

Figure 3: Summary of the experimental procedure to optimize the photopatterning of OPF/PEG-DA and CSMA hydrogels. The left section of the diagram illustrates the steps in photopatterning hydrogels in normal conditions (room air, with oxygen present), while the left section illustrates the use of an external nitrogen chamber to purge the system with nitrogen and displace any oxygen present before and during crosslinking.

Photopatterning of the CSMA polymer was attempted, and effects of crosslinking time, UV lamp intensity, and the presence or absence of oxygen on the photopatterned hydrogels investigated. The CSMA polymer solution, 90% w/w H_2O and 0.05% w/v D2959 photoinitiator, was prepared and injected into a microfluidic flow cell, which was either equilibrated with a nitrogen atmosphere 30 minutes prior or left in room air. CSMA hydrogels were photopatterned in a series of square blocks, with sizes ranging from 550 µm to 3000 µm. Crosslinking time was varied from 8 minutes to 12 minutes, and UV lamp intensity varied from 10.5 mW/cm^2 to 11.5 mW/cm^2. After crosslinking using a predefined set of the specified parameters, any hydrogels formed were excised from the flow cell and imaged under a dissecting scope (Leica), both immediately after crosslinking and after immersion for 24 hours in a solution of phosphate buffered saline. See Figure 4 for a summary of both OPF/PEG-DA and CSMA hydrogel chemistries.

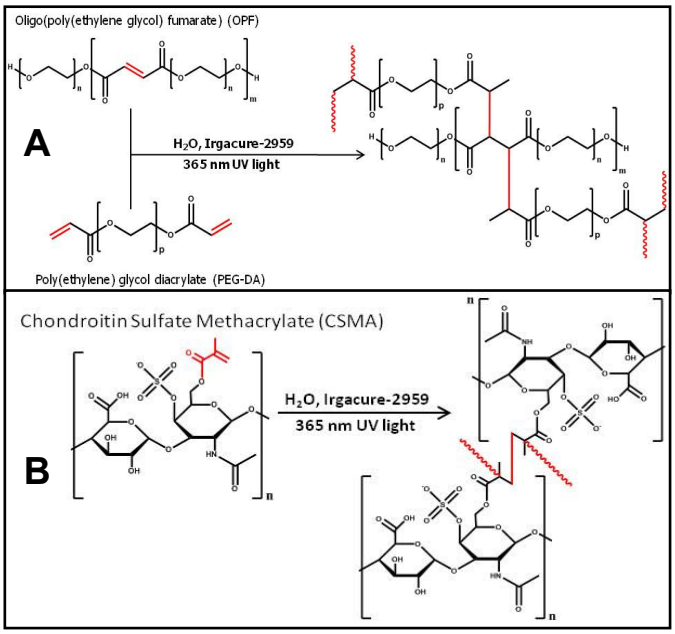

Figure 4: Summary of the crosslinking chemistries for both (a) OPF/PEG-DA hydrogels and (b) CSMA hydrogels.

System optimization: flow cell washing

During the serial photopatterning of different cell types, it would be necessary to completely remove cell populations in between crosslinking steps to ensure that no mixing between the populations occurred. In order to ensure that existing photopatterned gels would not obstruct removal of residual cell/polymer solution, polystyrene beads 10 μm in diameter (used in lieu of cells) were homogeneously dispersed at a concentration of 10×10^6 beads/mL in a polymer solution comprised OPF (M_n = 10,000 kDa) and PEG-DA (M_n = 3,400 kDa) (50% w/w OPF/PEG-DA, 75% w/w H_2O, 0.05% w/v D2959 photoinitiator). The crosslinking was performed in a controlled, oxygen-free environment to mitigate the inhibitive effects of oxygen on the crosslinking process. A prefabricated microfluidic flow cell was allowed to equilibrate with a nitrogen atmosphere, and after 30 minutes the polymer solution was injected into the flow cell. Hydrogels were photopatterned for 12 minutes under UV light (375 nm wavelength) and a nitrogen atmosphere. The hydrogels were photopatterned in an array of alternating square blocks, with block spacing varying from 100 μm to 750 μm. After photopatterning, the remaining bead/polymer solution was washed from the flow cell using an isotonic PEG solution, and the process was recorded using dark field microscopy. This process is illustrated in Figure 5.

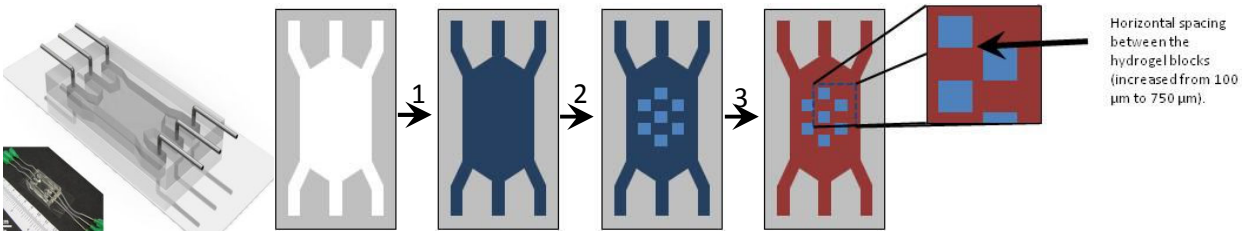

Figure 5: Simulated washing of cells from a microfluidic flow cell after crosslinking one set of OPF/PEG-DA hydrogels. (Left) Photograph and computer rendering of the new flow cell design. (Right) A summary of the optimization process: (1) Inject macromer solution (with polystyrene beads) into device (dark blue); (2) Photopattern hydrogel blocks (light blue); (3) Wash out residual macomer/bead solution with bead-free macromer solution of poly(ethylene glycol) (red).

System optimization: hydrogel lamination and demonstration interface stability and of interface separability through the incorporation of a degradable CSMA adhesive

A hydrogel tri-laminate consisting of two OPF/PEG-DA hydrogels with a CSMA hydrogel at the interface was created in order to demonstrate the inherent stability of the structure after swelling, and to show that the OPF/PEG-DA portions may be separated upon degradation of the CSMA interface. OPF/PEG-DA hydrogels (75% w/w H_2O, 0.05% w/v D2959) were photo-patterned for 15 minutes in a prefabricated PDMS flow cell. CSMA (90% w/w H_2O, 0.05% w/v D2959) was then injected into the flow cell and allowed to crosslink for 10 minutes. The laminate was then excised, the CSMA stained with dimethylmethylene blue (DMMB), and immersed in 1.75 mL of a chondroitinase buffer solution (pH of 8.0) to which 0.25 mL of a solution containing the enzyme chondroitin sulfate ABC lyase was added. CSMA control gels (90% w/w H_2O, 0.05% w/v D2959) were also created, stained with DMMB, placed in 2 mL of chondroitinase buffer solution, and incubated at 37^{o}C. The laminates and control gels were periodically monitored to check for complete degradation. Pre- and post-degradation images of the laminates were taken using an inverted Nikon TE2000U microscope and a digital camera.

To qualitatively study the interface of a laminate consisting of two differentially swollen hydrogels (similar to an OPF/PEG-DA/CSMA laminate), the methacrylated fluorophores rhodamine B and fluorescein were added to two OPF/PEG-DA gel solutions. The first solution consisted of OPF (molecular weight of 10,000 kDa) (OPF 10k) and PEG-DA to which a methacrylated fluorescein was added with a final concentration of 2.5 mM. A second gel

solution was likewise prepared, but with OPF 3.4k in place of OPF 10k and to which methacrylated rhodamine B was added to achieve a final concentration of 0.25 mM. A PDMS flow cell was placed into a larger PDMS chamber and flushed for 30 minutes with nitrogen gas. The OPF 10k gel solution was then injected into the flow cell and photo-patterned under a UV lamp. Afterwards, an isotonic solution of PEG 10k and PEG 20k (50% by mass, 75% w/w H_2O) was injected into the flow cell to wash out the remaining OPF 10k solution. The OPF 3.4k solution was subsequently injected and photo-patterned. Both gels were crosslinked for 12 minutes. The laminate was then excised and fluorescent images were obtained using a Leica MZ16F dissecting microscope.

Creation and degradation of a hydrogel tri-laminate with a degradable CSMA interface, and assessment of cell population segregation and viability before and after degradation

To determine the length of time required to separate hydrogel tri-laminate components, molding devices were constructed by placing a 1 mm-thick spacer of PDMS between two glass slides that contained a cavity to accommodate the polymer solution. The tri-laminate was created by successively crosslinking and subsequently masking a layer of PEG-DA, CSMA, and PEG-DA (90% w/w H_2O, 0.05% w/v D2959) under 365 nm light at 10.5 mW/cm^2 for 12 min, as shown in Figure 6. The hydrogels were divided into 1.5 mm wide sections and allowed to reach equilibrium swelling, whereupon they were added to a chondroitinase buffer solution (200 mM tris-HCl, 240 mM Na-acetate) containing the enzyme chondroitinase ABC

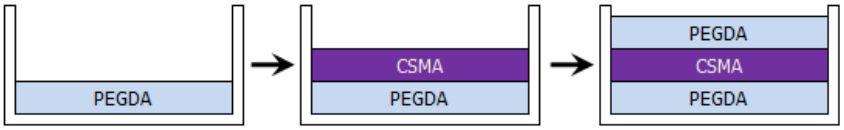

Figure 6: Creation of hydrogel tri-laminate with a degradable CSMA interface. Visual representation of the sequential patterning of the multi-layer hydrogel laminate, consisting of two PEGDA hydrogels with a CSMA interface (labeled). The laminate was later excised and the CSMA interface degraded with chondroitinase ABC.

at 0.25, 0.5, and 1 U/mL to assess degradation time.

To establish if cells retained viability after separation of the tri-culture laminate, the same experiment was repeated with encapsulated human mesenchymal stem cells (hMSC, passage 6; Texas A&M) inside the PEG-DA hydrogels at a density of 10×10^6 cells/mL. One tri-laminate included a group of cells in the first layer stained with Orange CMRA and in the second layer a group of cells stained with Green CMFDA (Invitrogen); these were visualized using fluorescence microscopy to ensure population segregation. After encapsulation, the sectioned laminates were allowed to culture for 1 day in growth media (alpha-MEM (Mediatech), 16.5% fetal bovine serum, 1% L-glutamine, and 1% glutamicin/amphotericin B) after which they were added to the chondroitinase buffer solution containing the enzyme chondroitinase ABC at 0.25, 0.5, and 1 U/mL. After separation of the PEG-DA layers, the gels were cultured for an additional day in growth media and their viability assessed with a LIVE/DEAD assay (Invitrogen) in conjunction with confocal microscopy.

RESULTS

CSMA hydrogel characterization: fold swelling ratio and degradation time

After synthesizing multiple batches of the the CSMA polymer, bulk crosslinking yielded hydrogels with fold swelling ratios ranging from 18 to 38 minutes and degradation times ranging from 80 to 210 minutes, depending on the polymer batch used. The degradation time of the hydrogel correlated reasonably well with the fold swelling ratio ($r^2 = 0.6103$); hydrogels with

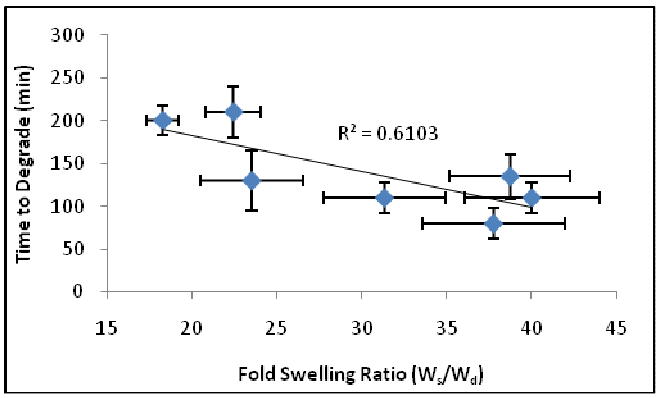

Figure 7: Plot of CSMA hydrogel degradation time as a function of fold swelling ratio. CSMA hydrogels with higher fold swelling ratios exhibited shorter degradation times, while CSMA hydrogels with lower values for F_s generally took a longer time to degrade.

higher fold swelling ratios generally exhibited shorter degradation times and hydrogels with lower fold swelling ratios took longer to degrade, as expected (Figure 7).

Hydrogel photopatterning optimization: OPF/PEG-DA and CSMA

A cross-sectional diagram of the PDMS microfluidic flow cell with and without the respective nitrogen chamber is shown in Figure 5. The dimensions of the OPF/PEG-DA hydrogels photopatterned were found to correlate strongly with the dimensions of the photomask to produce those hydrogels ($r^2 = 0.9987$ and $r^2 = 0.9927$ for hydrogels photopatterned with and without nitrogen, respectively) (Figure 8). The geometry of the hydrogel was easily adjusted by changing the photomask. Additionally, the feature fidelity and thickness was found to be significantly increased in the OPF/PEG-DA hydrogels photopatterned under nitrogen. Thicknesses of greater than 1 mm were obtained for hydrogels as small as 900 μm in width, and these thicknesses were maintained for all hydrogels photopatterned with nitrogen. Hydrogels photopatterned under nitrogen were also found to swell significantly less than those photopatterned in room air, suggesting a more highly crosslinked network.

The same set of experiments was repeated with CSMA hydrogels. Similarly to the results obtained with OPF/PEG-DA hydrogels, the dimensions of the photopatterned CSMA hydrogels

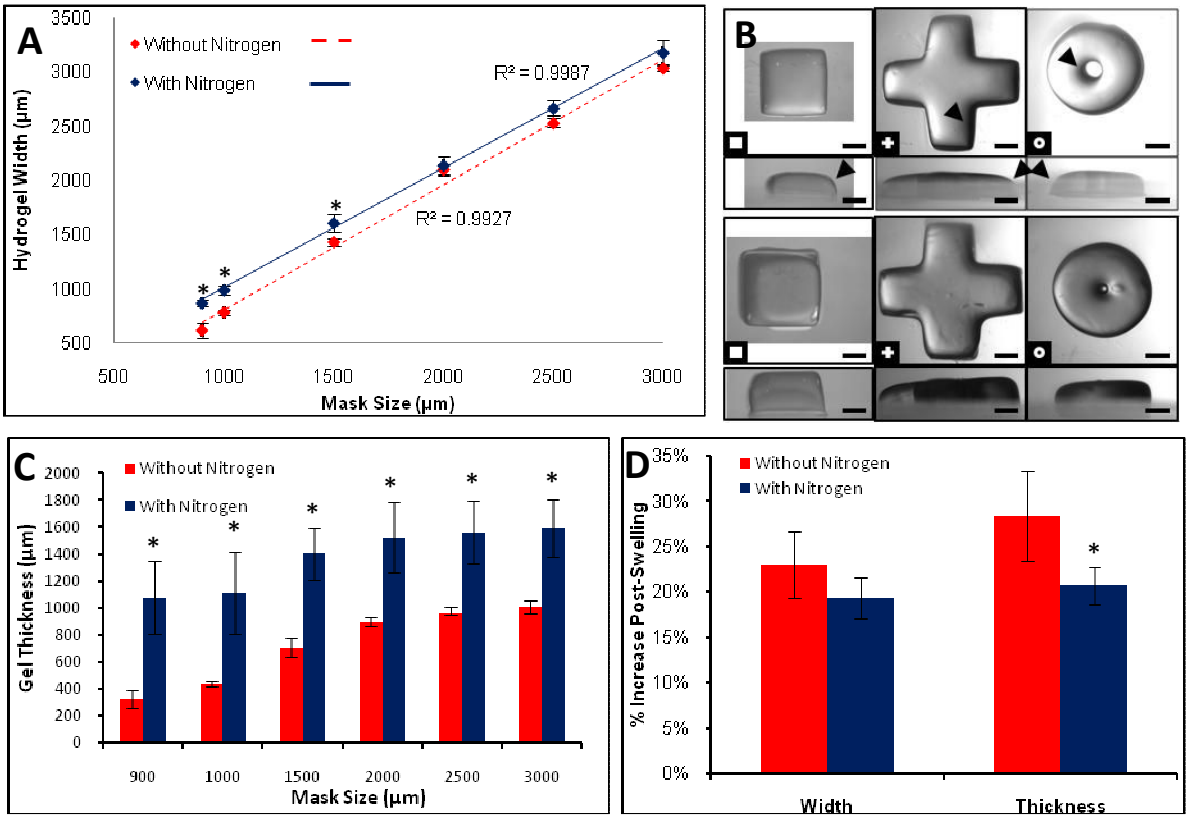

Figure 8: The effects of photopatterning under nitrogen on OPF/PEG-DA hydrogel thickness, patterning fidelity, and percent increase in size after swelling. (a) Hydrogel dimensions correlated well to the dimensions of the photomask used to pattern the gel, both with and without nitrogen. (b) Different hydrogel shapes are obtained by altering the geometries of the photomask (shown in the bottom left-hand corner of each image). Also, patterning OPF/PEG-DA hydrogels under nitrogen (bottom set of images) eliminated the presence of rounded corners and edges present in hydrogels photopatterned in room air (top set of images, noted by black arrows) and enhanced hydrogel features (scale bar = 1 mm). (c) Hydrogel thickness was significantly enhanced when patterned with nitrogen, with hydrogels as small as 900 µm exceeding thickness of 1 mm or more. (d) Hydrogels patterned with nitrogen increased significantly less in thickness than those patterned in room air, suggesting a more highly crosslinked network. n=3, error bars indicate ± standard deviation.

once again correlated strongly with the dimensions of the applied photomask (Figure 9). However, CSMA hydrogels could not be photopatterned at all without the use of the nitrogen chamber. The CSMA hydrogels that were photopatterned exceeded 1 mm in thickness, and gels as small as 650 µm across could be successfully photopatterned using these techniques. Additionally, detailed shapes and geometries could be obtained by altering the shape of the photomask used.

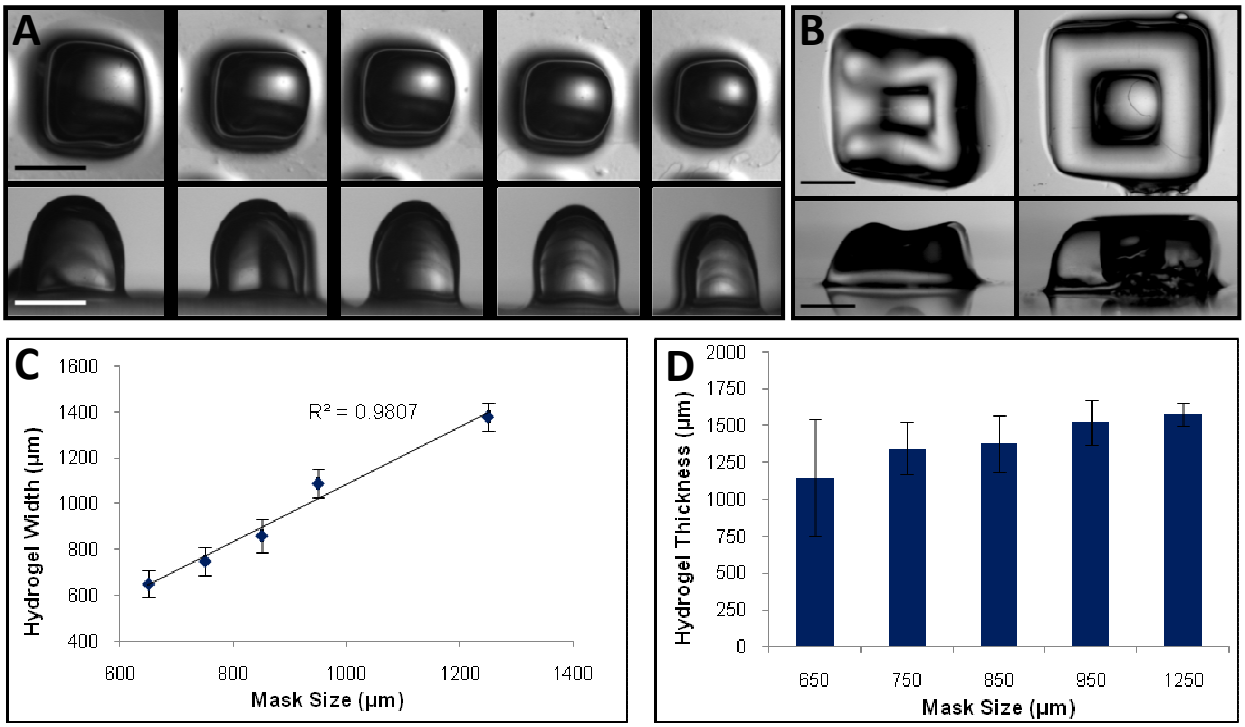

Figure 9: Photopatterning of CSMA hydrogels under nitrogen. (a) Top (first row) and side (second row) profiles of CSMA hydrogels ranging in size from 650 µm to 1250 µm (scale bar = 1 mm). (b) The geometry of the CSMA hydrogel could be adjusted by altering the shape of the photomask used; in this case, two different similar photomasks were used to achieve the same pattern, but the width of the structure was adjusted by varying the width of the transparent region on the photomask (scale bar = 1 mm). (c) CSMA hydrogel dimensions were found to correlate well with the dimensions of the photomask used, and (d) CSMA hydrogel thickness exceeded 1 mm in hydrogels as small as 650 µm across.

System optimization: flow cell washing

In order to ensure that different cell populations would not mix in between crosslinking steps, it was necessary to devise a new microfluidic flow cell design that would facilitate the complete removal of residual cells. The final flow cell design was then implemented in all further experiments, and is shown in Figure 5. After varying the distance between photopatterned hydrogels, it was found that the large majority of beads could be cleared from the flow cell after patterning with a minimum horizontal spacing between 100 µm and 250 µm, as shown in Figure 10.

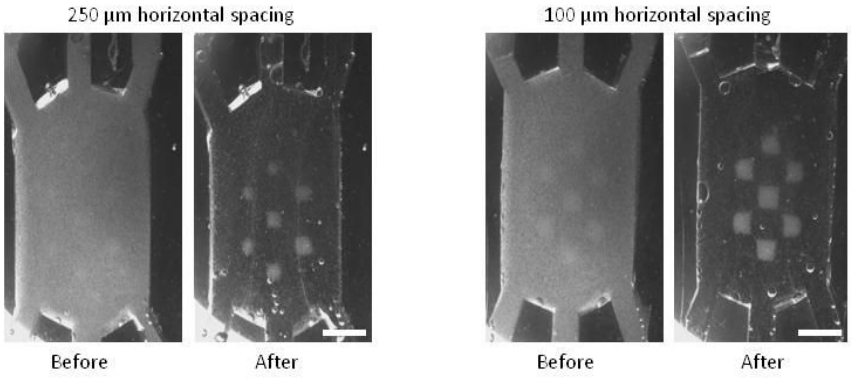

Figure 10: Simulated washing of cells from a microfluidic flow cell after crosslinking one set of OPF/PEG-DA hydrogels. Results of the optimization with 250 µm and 100 µm spacing between hydrogels. All the beads were successfully cleared from the flow cell when hydrogels were spaced as close as 100 µm (scale bar = 1 mm).

System optimization: hydrogel lamination and demonstration interface stability and of interface separability through the incorporation of a degradable CSMA adhesive

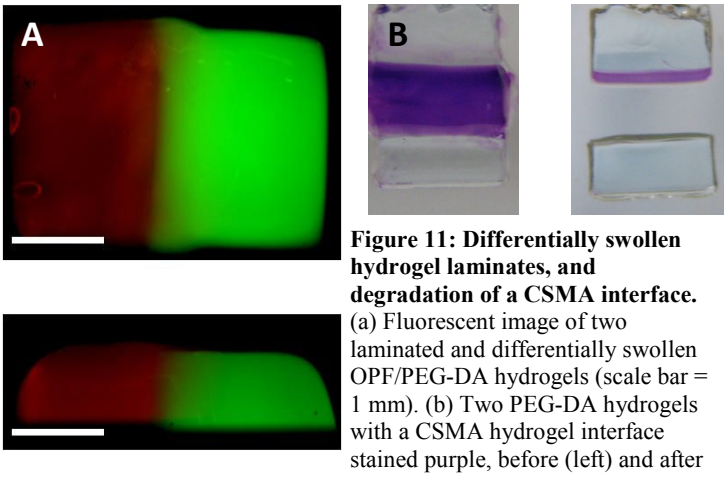

Figure 11: Differentially swollen hydrogel laminates, and degradation of a CSMA interface. (a) Fluorescent image of two laminated and differentially swollen OPF/PEG-DA hydrogels (scale bar = 1 mm). (b) Two PEG-DA hydrogels with a CSMA hydrogel interface stained purple, before (left) and after (right) degradation of the CSMA.

After photopatterning and visualization with the acrylated fluorescent dye, the interface between the two differentially swollen photopatterned OPF hydrogels remained stable (Figure 11a). CSMA was successfully laminated between two PEG-DA hydrogels as well, and after swelling the hydrogel construct remained stable. Upon addition of chondroitinase, the CSMA interface dissolved, leaving the two PEG-DA hydrogels intact (Figure 11b).

Creation and degradation of a hydrogel tri-laminate with a degradable CSMA interface, and assessment of cell population segregation and viability before and after degradation

CSMA hydrogels were found to degrade readily upon exposure to chondroitinase ABC lyase, and lamination to PEG-DA gels did not appreciably affect CSMA degradative properties. PEG-DA gels remained laminated after swelling and were separated upon addition of chondroitinase. The time required to separate the two PEG-DA gels varied from less than 1 hour for 1 U/mL chondroitinase to over 4 hours at 0.25 U/mL. After visualization with fluorescence microscopy, the two hMSC populations (distinguished with Cell Tracker Green CMFDA and Orange CMRA) remained separated after the encapsulation process (Figure 12). Additionally, as shown in Figure 13, cell viability was maintained throughout the process of encapsulation and after separation, with no observable decrease in viability regardless of the concentration of enzyme used to degrade the CSMA interface of the tri-laminate.

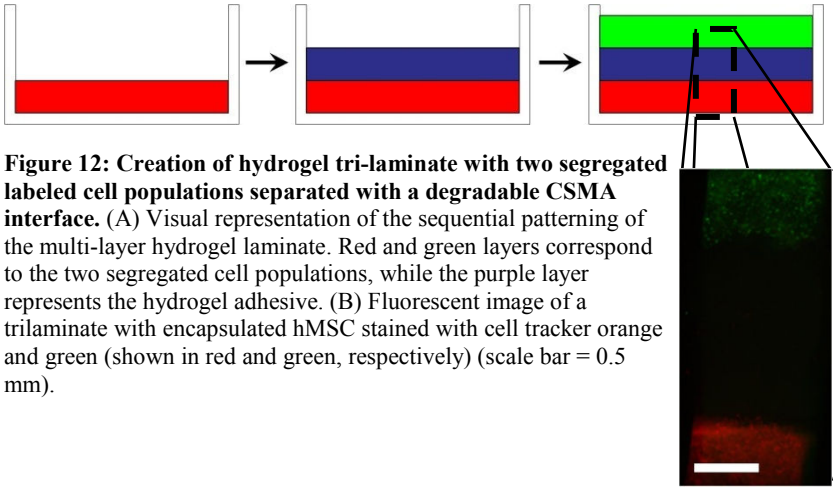

Figure 12: Creation of hydrogel tri-laminate with two segregated labeled cell populations separated with a degradable CSMA interface. (A) Visual representation of the sequential patterning of the multi-layer hydrogel laminate. Red and green layers correspond to the two segregated cell populations, while the purple layer represents the hydrogel adhesive. (B) Fluorescent image of a trilaminate with encapsulated hMSC stained with cell tracker orange and green (shown in red and green, respectively) (scale bar = 0.5 mm).

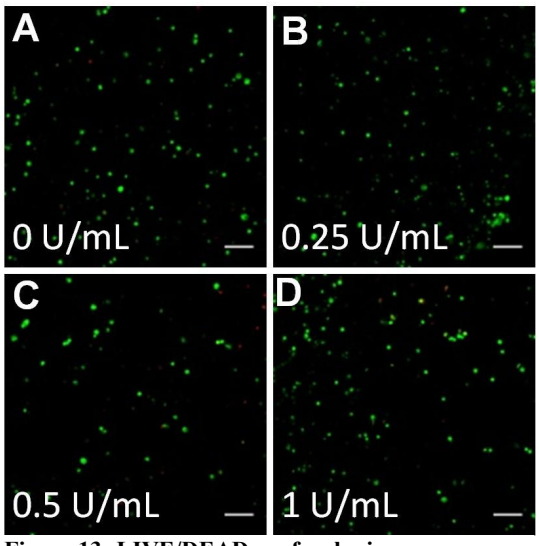

Figure 13: LIVE/DEAD confocal microscopy images of cells (A) before degradation of the CSMA interface and after using (B) 0.25 U/mL, (C) 0.5 U/mL, and (D) 1 U/mL of chondroitinase. Green indicates viable cells, and red indicates dead. Scale bar = 100 μm.

DISCUSSION

The utilization of artificial biomimetic scaffolds such as hydrogels in the formation of 3D tissue-engineered constructs has been accomplished in a variety of ways and is useful for the creation of *in vitro* tissue models enabling the study of 3D cellular physiology[27]. A better understanding of this physiology will result in more effective tissue-replacement therapies and techniques, such as the engineering of stem cells outside of the body before implantation to ensure successful engraftment[1]. Additionally, by combining 3D cell encapsulation techniques with co-culture, the manner in which different cell populations interact and influence one another can be determined. Current transwell co-culture techniques are limited in their inability to reproduce 3D tissue physiology. While several techniques exist that allow for the co-culture of multiple cell types in 3D[11, 44-47], they are generally very specialized in their implementation and do not allow for the recovery of viable segregated cell populations for *in vitro* post-culture analysis. The system developed here overcomes both of these obstacles, while maintaining the ability to pattern cells in a tunable 3D microenvironment similar to native tissues and tissue components.

The photopatterning technologies and system developed here represent the very first working prototype of its kind. The photolithographic methods of patterning hydrogel structures yield architectures whose dimensions correlate strongly with those of the applied photomask. This suggests that the system can be easily calibrated, depending on the size and type of geometry desired. Additionally, by altering the shape of the photomask, any number of hydrogel shapes is obtainable. This consequential versatility and ease of use is a product of the photopatterning technique[24, 28] and thus, by extension, an inherent property of our system.

Alteration of hydrogel shape could be employed to distinguish between different cell populations housed in the microstructure; this would be especially useful if the system is expanded to include the culturing of three or more different cell populations.

The introduction of a nitrogen chamber and photopatterning under a nitrogen atmosphere resulted in hydrogels with thicknesses greater than 1 mm and very high aspect ratios. These results are consistent with previous studies detailing the inhibitory effects of oxygen on the photopolymerization process[38]. The thicknesses obtained using these photopatterning procedures are very similar to those found in native tissue environments, an important attribute for an *in vitro* model capable of accurately representing an *in vivo* environment. The ability to obtain relatively high (>1 mm) thicknesses with micropatterned hydrogels makes this system unique from previous, similar photopatterning techniques[11, 35-37, 40]. Additionally, the fact that the system allows for the photopatterning of hydrogels on the microscale makes it ideal for studying tissue microenvironments[27] and diffusion-limited paracrine signaling effects, as the effects of these endogenous signals lose their potency with distance from the secreting cell due to their dilution in the surrounding media.

The new microfluidic flow cell design allows for the successful removal of residual polymer solution containing cell-like components. After visualization a thin, uniform coating of polystyrene beads was noticed along the bottom of the flow cell. However, this coating was later found to be due to the settling of the beads along the surface of the coverglass – it is anticipated that when actual cells are used in place of these polystyrene beads, this settling effect will be far less significant, as the cells' density differs little from that of the aqueous polymer solution. The successful removal of residual cells from the flow cell after each crosslinking step, as well as the volume of washing solution necessary to remove them, depends on both the design of the flow

cell as well as the obstruction to flow caused by the hydrogel structure occupying the central chamber. The fact that different hydrogel shapes may alter the flow in different ways highlights an important limitation in the types and shapes of structures that can be created using this system. Some geometries may impede the removal of residual cells causing inhomogeneity in the encapsulation of subsequent cell populations. This problem could be circumvented by changing the design of the flow cell; this task is made easier by the fact that the flow cells can be easily fabricated with a relatively high throughput, as they are simple PDMS castings bonded to a piece of coverglass.

Differentially swollen hydrogels, once laminated together by sequential photopatterning, retained a stable interface that did not rupture after swelling. These results suggest that the system could be used to sequentially pattern hydrogel structures that contain not only different cell types but also different types of crosslinked hydrogels, as long as the necessary vinyl moiety is present in the constituent polymer. This would impart additional versatility to the system, as it would allow for the study of differing extracellular matrix components on cell growth and behavior. The CSMA hydrogel synthesis yielded a material that was successfully laminated with an existing OPF/PEG-DA hydrogel through photocrosslinking and further integrated into a hydrogel structure with multiple components. Upon addition of the enzyme chondroitinase ABC the CSMA interface dissolved, leaving the other hydrogel components intact and completely separate. After repeating these experiments with encapsulated cells, the CSMA degradation process appeared to have no immediate detrimental effects on cell viability after separation, and cell populations remained separated and distinct throughout the encapsulation process. This is especially important, as the successful recovery of viable cells after culture will allow for further experimentation on those populations.

One commonly employed method of non-contact, separable cell co-culture is the transwell system. Transwell works by providing two separated surfaces for cell growth in the same well, with one cell population plated on a removable membrane permeable to soluble factor signaling molecules. This versatile system has been used in the past to elucidate the effects of paracrine signaling and cross-talk between various cell populations with notable success[48-50]. However, transwell culture is restricted to two dimensions, and thus is limited in its ability to accurately simulate native tissue physiology. More advanced 3D cell co-culture systems are often uniquely specialized in their applications and unable to allow for the facile separation and post-culture analysis of segregated cell types[44-47]. The system developed here represents a significant advantage over both traditional transwell co-culture methods and current 3D co-culture systems in that it provides the physiologically representative 3D environment for cell growth, is versatile enough to answer a variety of important biological questions concerning stem cell growth and development, and allows for the sequential separation and recovery of viable cell populations through the incorporation ofone or more stimulus-responsive adhesives. Additionally, the system can be potentially further tailored to more accurately represent tissue physiology by incorporating a multitude of biofactors, peptides, and other moieties into the hydrogel network[14-15].

CONCLUSION

The completion of this project represents the development of a novel hydrogel fabrication system that (a) allows for the sequential crosslinking of a hydrogel structure with various and easily alterable geometries; (b) produces hydrogel structures that are microns in width while still retaining thicknesses of greater than 1 mm, which would allow for the diffusion-limited exchange of soluble factors between cell populations while closely representing the dimensions of native tissue; (c) allows for the incorporation of different types of hydrogels into one cohesive architecture that retains its structural integrity over time. A direct consequence of (c) is the incorporation of the CSMA hydrogel as a temporary adhesive holding multiple hydrogels in close proximity. Taken together, the aspects of this system make it well suited for implementation in the production of a separable 3D co-culture system for the study of paracrine signaling effects between cell populations. Its inherent utility and versatility make it an ideal tissue model, and the information it will assist in obtaining from future co-culture studies will help to elucidate the biological mechanisms of stem cell development that could allow for the successful implementation of regenerative medicine therapies.

REFERENCES

1. Griffith LG, Swartz MA. Capturing complex 3D tissue physiology in vitro. *Nature Reviews Molecular Cell Biology.* 2006;7(3):211-224.

2. Nelson CM, Tien J. Microstructured extracellular matrices in tissue engineering and development. *Current Opinion in Biotechnology.* 2006;17(5):518-523.

3. Griffith LG, Naughton G. Tissue engineering - Current challenges and expanding opportunities. *Science.* 2002;295(5557):1009-+.

4. Discher DE, Mooney DJ, Zandstra PW. Growth Factors, Matrices, and Forces Combine and Control Stem Cells. *Science.* 2009;324(5935):1673-1677.

5. Engler AJ, Sen S, Sweeney HL, Discher DE. Matrix elasticity directs stem cell lineage specification. *Cell.* 2006;126(4):677-689.

6. Pampaloni F, Reynaud EG, Stelzer EHK. The third dimension bridges the gap between cell culture and live tissue. *Nature Reviews Molecular Cell Biology.* 2007;8:839-845.

7. Jongpaiboonkit L, King WJ, Lyons GE, et al. An adaptable hydrogel array format for 3-dimensional cell culture and analysis. *Biomaterials.* 2008;29(23):3346-3356.

8. Griffith LG. Emerging design principles in Biomaterials and scaffolds for tissue engineering. *Reparative Medicine: Growing Tissues and Organs.* 2002;961:83-95.

9. Hubbell JA. Materials as morphogenetic guides in tissue engineering. *Current Opinion in Biotechnology.* 2003;14(5):551-558.

10. Koh WG, Revzin A, Pishko MV. Poly(ethylene glycol) hydrogel microstructures encapsulating living cells. *Langmuir.* 2002;18(7):2459-2462.

11. Liu VA, Bhatia SN. Three-dimensional photopatterning of hydrogels containing living cells. *Biomedical Microdevices.* 2002;4(4):257-266.

12. Albrecht DR, Tsang VL, Sah RL, Bhatia SN. Photo- and electropatterning of hydrogel-encapsulated living cell arrays. *Lab Chip.* 2005;5(1):111-118.

13. Temenoff JS, Park H, Jabbari E, et al. Thermally cross-linked oligo(poly(ethylene glycol) fumarate) hydrogels support osteogenic differentiation of encapsulated marrow stromal cells in vitro. *Biomacromolecules.* Jan-Feb 2004;5(1):5-10.

14. Moon JJ, Hahn MS, Kim I, Nsiah BA, West JL. Micropatterning of Poly(Ethylene Glycol) Diacrylate Hydrogels with Biomolecules to Regulate and Guide Endothelial Morphogenesis. *Tissue Eng. Part A.* Mar 2009;15(3):579-585.

15. Koh WG, Itle LJ, Pishko MV. Molding of hydrogel multiphenotype cell microstructures to create microarrays. *Analytical Chemistry.* 2003;75(21):5783-5789.

16. Bulpitt P, Aeschlimann D. New strategy for chemical modification of hyaluronic acid: Preparation of functionalized derivatives and their use in the formation of novel biocompatible hydrogels. *Journal of Biomedical Materials Research.* Nov 1999;47(2):152-169.

17. Cai SS, Liu YC, Shu XZ, Prestwich GD. Injectable glycosaminoglycan hydrogels for controlled release of human basic fibroblast growth factor. *Biomaterials.* Oct 2005;26(30):6054-6067.

18. Tsai MF, Tsai HY, Peng YS, Wang LF, Chen JS, Lu SC. Characterization of hydrogels prepared from copolymerization of the different degrees of methacrylate-grafted chondroitin sulfate macromers and acrylic acid. *J. Biomed. Mater. Res. Part A.* Mar 2008;84A(3):727-739.

19. Huang SJ, Wang JM, Tseng SC, Wang LF, Chen JS. Controlled immobilization of chondroitin sulfate in polyacrylic acid networks. *J. Biomater. Sci.-Polym. Ed.* 2007;18(1):17-34.

20. Wang LF, Shen SS, Lu SC. Synthesis and characterization of chondroitin sulfate-methacrylate hydrogels. *Carbohydr. Polym.* Jun 2003;52(4):389-396.

21. Bryant SJ, Davis-Arehart KA, Luo N, Shoemaker RK, Arthur JA, Anseth KS. Synthesis and characterization of photopolymerized multifunctional hydrogels: Water-soluble poly(vinyl alcohol) and chondroitin sulfate macromers for chondrocyte encapsulation. *Macromolecules.* Sep 2004;37(18):6726-6733.

22. Hamai A, Hashimoto N, Mochizuki H, et al. Two distinct chondroitin sulfate ABC lyases - An endoeliminase yielding tetrasaccharides and an exoeliminase preferentially acting on oligosaccharides. *J. Biol. Chem.* Apr 1997;272(14):9123-9130.

23. Bruzewicz DA, McGuigan AP, Whitesides GM. Fabrication of a modular tissue construct in a microfluidic chip. *Lab Chip.* 2008;8(5):663-671.

24. Khademhosseini A, Langer R, Borenstein J, Vacanti JP. Microscale technologies for tissue engineering and biology. *Proceedings of the National Academy of Sciences of the United States of America.* Feb 2006;103(8):2480-2487.

25. Yeh J, Ling YB, Karp JM, et al. Micromolding of shape-controlled, harvestable cell-laden hydrogels. *Biomaterials.* Nov 2006;27(31):5391-5398.

26. McGuigan AP, Bruzewicz DA, Glavan A, Butte M, Whitesides GM. Cell Encapsulation in Sub-mm Sized Gel Modules Using Replica Molding. *Plos One.* 2008;3(5).

27. Tsang VL, Bhatia SN. Three-dimensional tissue fabrication. *Advanced Drug Delivery Reviews.* 2004;56(11):1635-1647.

28. Voldman J, Gray ML, Schmidt MA. Microfabrication in biology and medicine. *Annu. Rev. Biomed. Eng.* 1999;1:401-425.

29. Khademhosseini A, Langer R. Microengineered hydrogels for tissue engineering. *Biomaterials.* 2007;28:5087-5092.

30. Tsang VL, Chen AA, Cho LM, et al. Fabrication of 3D hepatic tissues by additive photopatterning of cellular hydrogels. *Faseb J.* Mar 2007;21(3):790-801.

31. Karp JM, Yeo Y, Geng WL, et al. A photolithographic method to create cellular micropatterns. *Biomaterials.* 2006;27(27):4755-4764.

32. Bryant SJ, Cuy JL, Hauch KD, Ratner BD. Photo-patterning of porous hydrogels for tissue engineering. *Biomaterials.* 2007;28(19):2978-2986.

33. Chung SE, Park W, Park H, Yu K, Park N, Kwon S. Optofluidic maskless lithography system for real-time synthesis of photopolymerized microstructures in microfluidic channels. *Applied Physics Letters.* 2007;91(4).

34. Cheung YK, Gillette BM, Zhong M, Ramcharan S, Sia SK. Direct patterning of composite biocompatible microstructures using microfluidics. *Lab Chip.* 2007;7(5):574-579.

35. Arcaute K, Mann BK, Wicker RB. Stereolithography of three-dimensional bioactive poly(ethylene glycol) constructs with encapsulated cells. *Annals of Biomedical Engineering.* 2006;34(9):1429-1441.

36. Nelson CM, Inman JL, Bissell MJ. Three-dimensional lithographically defined organotypic tissue arrays for quantitative analysis of morphogenesis and neoplastic progression. *Nature Protocols.* 2008;3(4):674-678.

37. Lee SH, Moon JJ, West JL. Three-dimensional micropatterning of bioactive hydrogels via two-photon laser scanning photolithography for guided 3D cell migration. *Biomaterials.* 2008;29(20):2962-2968.

38. Decker C, Jenkins AD. Kinetic Approach of O-2 Inhibition in Ultraviolet-Induced and Laser-Induced Polymerizations. *Macromolecules.* 1985;18(6):1241-1244.

39. Jo S, Shin H, Shung AK, Fisher JP, Mikos AG. Synthesis and characterization of oligo(poly(ethylene glycol) fumarate) macromer. *Macromolecules.* 2001;34(9):2839-2844.

40. Hahn MS, Taite LJ, Moon JJ, Rowland MC, Ruffino KA, West JL. Photolithographic patterning of polyethylene glycol hydrogels. *Biomaterials.* 2006;27(12):2519-2524.

41. McDonald JC, Whitesides GM. Poly(dimethylsiloxane) as a material for fabricating microfluidic devices. *Acc Chem Res.* Jul 2002;35(7):491-499.

42. Desai SP, Freeman DM, Voldman J. Plastic masters-rigid templates for soft lithography. *Lab on a Chip.* 2009;9(11):1631-1637.

43. Jackman RJ, Duffy DC, Cherniavskaya O, Whitesides GM. Using elastomeric membranes as dry resists and for dry lift-off. *Langmuir.* 1999;15(8):2973-2984.

44. Trkov S, Eng G, Di Liddo R, Parnigotto PP, Vunjak-Novakovic G. Micropatterned three-dimensional hydrogel system to study human endothelial - mesenchymal stem cell interactions. *J. Tissue Eng. Regen. Med.* Apr 2010;4(3):205-215.

45. Canton I, Cole DM, Kemp EH, et al. Development of a 3D Human In Vitro Skin Co-Culture Model for Detecting Irritants in Real-Time. *Biotechnol. Bioeng.* Aug 2010;106(5):794-803.

46. Liu TJ, Lin BC, Qin JH. Carcinoma-associated fibroblasts promoted tumor spheroid invasion on a microfluidic 3D co-culture device. *Lab Chip.* 2010;10(13):1671-1677.

47. Bauer M, Su G, Beebe DJ, Friedl A. 3D microchannel co-culture: method and biological validation. *Integr. Biol.* 2010;2(7-8):371-378.

48. Spector JA, Greenwald JA, Warren SM, et al. Co-culture of osteoblasts, with immature dural cells causes an increased rate and degree of osteoblast differentiation. *Plastic and Reconstructive Surgery.* Feb 2002;109(2):631-642.

49. Zoumpopoulou G, Tsakalidou E, Dewulf J, Pot B, Grangette C. Differential crosstalk between epithelial cells, dendritic cells and bacteria in a co-culture model. *Int. J. Food Microbiol.* Apr 2009;131(1):40-51.

50. Boyera N, Cavey D, Delamadeleine F, Bouclier M, Hensby C, Shroot B. A NOVEL IN-VITRO MODEL FOR THE STUDY OF HUMAN KERATINOCYTE LEUKOCYTE INTERACTIONS UNDER AUTOLOGOUS CONDITIONS. *Br. J. Dermatol.* Nov 1993;129(5):521-529.